Both Inducible Nitric Oxide Synthase and NADPH Oxidase Contribute to the Control of Virulent Phase I *Coxiella burnetii* Infections

Robert E. Brennan, Kasi Russell, Guoquan Zhang and James E. Samuel

***Infect. Immun.* 2004, 72(11):6666. DOI: 10.1128/IAI.72.11.6666-6675.2004.**

INFECTION AND IMMUNITY, Nov. 2004, p. 6666–6675 Vol. 72, No. 11
0019-9567/04/$08.00+0 DOI: 10.1128/IAI.72.11.6666–6675.2004

Both Inducible Nitric Oxide Synthase and NADPH Oxidase Contribute to the Control of Virulent Phase I *Coxiella burnetii* Infections

Robert E. Brennan, Kasi Russell, Guoquan Zhang, and James E. Samuel*

Department of Medical Microbiology and Immunology, Texas A&M University System Health Science Center, College Station, Texas

Received 29 February 2004/Returned for modification 15 April 2004/Accepted 14 July 2004

Host control of *Coxiella burnetii* infections is believed to be mediated primarily by activated monocytes/macrophages. The activation of macrophages by cytokines leads to the production of reactive oxygen intermediates (ROI) and reactive nitrogen intermediates (RNI) that have potent antimicrobial activities. The contributions of ROI and RNI to the inhibition of *C. burnetii* replication were examined in vitro by the use of murine macrophage-like cell lines and primary mouse macrophages. A gamma interferon (IFN-γ) treatment of infected cell lines and primary macrophages resulted in an increased production of nitric oxide (NO) and hydrogen peroxide (H_2O_2) and a significant inhibition of *C. burnetii* replication. The inhibition of replication was reversed in the murine cell line J774.16 upon the addition of either the inducible nitric oxide synthase (iNOS) inhibitor N^G-monomethyl-L-arginine (N^GMMLA) or the H_2O_2 scavenger catalase. IFN-γ-treated primary macrophages from iNOS$^{-/-}$ and p47$^{phox-/-}$ mice significantly inhibited replication but were less efficient at controlling infection than IFN-γ-treated wild-type macrophages. To investigate the contributions of ROI and RNI to resistance to infection, we performed in vivo studies, using C57BL/6 wild-type mice and knockout mice lacking iNOS or p47^{phox}. Both iNOS$^{-/-}$ and p47$^{phox-/-}$ mice were attenuated in the ability to control *C. burnetii* infection compared to wild-type mice. Together, these results strongly support a role for both RNI and ROI in the host control of *C. burnetii* infection.

Coxiella burnetii, the etiologic agent of Q fever, is an obligate intracellular bacterium. Q fever is a zoonosis that is found worldwide, with a broad host range that includes wild and domestic mammals, birds, arthropods, and humans (9). For humans, the primary route of infection is through the inhalation of contaminated aerosols associated with domestic ruminants (40). Following inhalation, the organism is taken up primarily by resting alveolar macrophages, replicates to high numbers, and disseminates to a variety of tissues upon host cell rupture. Q fever can manifest as an acute illness that resembles influenza or as a chronic illness that is most often characterized by endocarditis. Clinically, acute Q fever is generally a self-limiting febrile illness that can be readily treated with tetracyclines to accelerate recovery (49). Conversely, chronic Q fever is refractory to antibiotics, with significant mortality rates even when patients receive the most effective treatment currently available, which is doxycycline plus chloroquine for at least 18 months (51).

C. burnetii has the unique ability among bacteria to replicate within an acidified vacuole of a resting host cell despite the presence of toxic host factors such as acid hydrolases and defensins (4). Although both infection with viable *C. burnetii* and vaccination with killed whole-cell *C. burnetii* lead to the development of humoral and cell-mediated immune responses, the host defense appears to be dependent on the enhanced microbicidal mechanisms of macrophages that are activated by specifically sensitized T cells (7, 33, 36). Previous studies have demonstrated that the activation of guinea pig monocytes, THP-1 monocytes, L929 murine fibroblasts, and primary mouse macrophages by gamma interferon (IFN-γ) results in the inhibition of *C. burnetii* replication (20, 31, 32, 54, 57). However, only a few studies have been done to determine the mechanisms used by either professional or nonprofessional phagocytes to control *C. burnetii* replication. Dellecasagrande et al. reported that infected THP-1 monocytes stimulated with IFN-γ were able to inhibit phase I *C. burnetii* replication and suggested that a tumor necrosis factor alpha-driven apoptotic mechanism may be involved (20). Recently, Howe et al. demonstrated that nitric oxide (NO) reversibly inhibits the replication of avirulent phase II *C. burnetii* in IFN-γ-treated L929 murine fibroblasts (32). Zamboni and Rabinovitch reported that phase II *C. burnetii* induced NO in primary mouse macrophages and that this NO was partially responsible for reducing the numbers of *C. burnetii* organisms in these cells. They also demonstrated that IFN-γ-treated primary macrophages from inducible nitric oxide synthase-negative (iNOS$^{-/-}$) mice controlled phase II *C. burnetii* infections, which suggests that NO-independent mechanisms were also involved (57).

IFN-γ-activated macrophages are capable of generating reactive oxygen intermediates (ROI) and reactive nitrogen intermediates (RNI) that enhance the ability of these cells to control the growth of intracellular organisms. IFN-γ stimulation results in the activation of NADPH oxidase and iNOS. NADPH oxidase reduces oxygen to a superoxide anion (O_2^-), which can then enter the phagosome and be changed to hydrogen peroxide (H_2O_2) by a dismutase (17). iNOS synthesizes NO from L-arginine and oxygen. Reactive oxygen and nitrogen intermediates can inactivate [4Fe-4S] cluster-containing enzymes, damage DNA, and oxidize cellular membranes and enzymes (21, 27, 56). The antimicrobial activities of these in-

* Corresponding author. Mailing address: Department of Medical Microbiology and Immunology, Texas A&M University System Health Science Center, College Station, TX 77843-1114. Phone: (979) 862-1684. Fax: (979) 845-3479. E-mail: jsamuel@tamu.edu.

termediates have been demonstrated in vitro as well as in vivo. *Mycobacterium tuberculosis*, *Leishmania donovani*, and *Rickettsia conorii* have all been shown to be susceptible to H_2O_2 killing in vitro (22, 34, 43). Mice lacking gp91^{phox}, which results in an NADPH oxidase deficiency, have an increased susceptibility to *M. tuberculosis* and *L. donovani* infections (2, 44). Mice lacking a functional iNOS were more susceptible to a challenge with virulent *M. tuberculosis* and died earlier after the challenge than did wild-type mice (38, 52). Also, the inhibition of iNOS resulted in a more rapid progression of chronic tuberculosis in wild-type mice (38). While prior studies have investigated the role of NO in controlling phase II *C. burnetii* infections in vitro, the goal of this study was to evaluate the roles that RNI and ROI play in the inhibition of virulent phase I *C. burnetii* infections in vitro and in vivo. To accomplish this goal, we conducted experiments in vitro, using J774 macrophage-like cell lines and primary macrophages from iNOS and p47^{phox} knockout (KO) mice, and in vivo challenge experiments, using iNOS and p47^{phox} KO mice.

MATERIALS AND METHODS

Macrophage killing experiments. (i) Reagents. Murine recombinant IFN-γ, hypoxanthine, and xanthine oxidase were purchased from Calbiochem (La Jolla, Calif.). Griess reagent, N^G-monomethyl-L-arginine, catalase, horseradish peroxidase (HRPO), phenol red, and Hanks' balanced salt solution were purchased from Sigma (St. Louis, Mo.). Experiments with macrophages were conducted in a biosafety level III laboratory.

(ii) J774 mouse macrophage experiments. Two murine phagocytic cell lines—J774.16, a strong oxidative burst-competent cell line (18), and J774D.9, which fails to generate an oxidative burst after phorbol myristate acetate stimulation (24)—were assessed for the ability to control *C. burnetii* replication with and without activation by IFN-γ. Hypoxanthine/xanthine oxidase (HX/XO) (an ROI donor) (12), catalase, and N^G-monomethyl-L-arginine (NMMLA) (a nitric oxide synthase inhibitor) (30) were included to determine the effects of ROI and RNI on bacterial replication. Briefly, cells were plated at 10^5/ml in 24- or 96-well tissue culture plates and then allowed to adhere for 4 h. Macrophages were infected with purified *C. burnetii* (Nine Mile, phase I, RSA 493) at a multiplicity of infection of 35:1, incubated overnight at 37°C in 5% CO_2, and then washed three times with warm medium to remove any uninternalized bacteria. Infected cells were then left untreated or were treated with IFN-γ (100 U/ml) alone or in combination with 1 mM NMMLA, 100 μM catalase, or 250 μM/30 μM HX/XO on days 1, 2, 3, 4, and 5 postinoculation. The ability of *C. burnetii* to replicate in these cells was assessed at 2, 4, and 6 days postinfection. The generation of NO and H_2O_2 was detected spectrophotometrically by the use of Griess reagent (25) and by the horseradish peroxidase-dependent oxidation of phenol red (47), respectively, in 96-well plates. The replication of *C. burnetii* was monitored by real-time PCR as previously described (14), using cells harvested from 24-well plates. Cell viability was determined by trypan blue exclusion.

(iii) Primary macrophage experiments. Peritoneal macrophages were harvested from C57BL/6, p47$^{phox-/-}$ (C57BL/6), and iNOS$^{-/-}$ (C57BL/6) mice (Taconi Farms Inc., Germantown, N.Y.) to obtain macrophages that were competent in both respiratory burst and nitric oxide production and macrophages that lacked a functional respiratory burst or nitric oxide production. Resident peritoneal macrophages (PMϕ) were collected by washing the peritoneal cavity of CO_2-euthanized mice with 6 ml of cold RPMI containing 10% fetal bovine serum. The cells were plated in 24- and 96-well tissue culture plates at 2×10^5 cells/well in cold RPMI containing 10% fetal bovine serum, 1% L-glutamine, 5% L-cell medium, and 1% penicillin-streptomycin and were allowed to adhere for 24 h at 37°C in 5% CO_2.

Primary macrophages were infected with purified *C. burnetii* (Nine Mile, phase I, RSA 493) at a multiplicity of infection of 35:1, incubated overnight at 37°C in 5% CO_2, and then washed three times with warm medium to remove any uninternalized bacteria. Infected cells were then treated with IFN-γ (100 U/ml) or were left untreated.

***C. burnetii* infection in mice.** C57BL/6, p47$^{phox-/-}$ (C57BL/6), and iNOS$^{-/-}$ (C57BL/6) mice (Taconi Farms Inc.) were challenged intraperitoneally with 10^4 or 10^7 phase I *C. burnetii* cells suspended in phosphate-buffered saline. The mice were observed daily for morbidity and mortality for 28 days postchallenge. Body weights were measured on days 14 and 28 postchallenge. On days 14 and 28 postchallenge, the mice were euthanized by the use of CO_2, and their spleens were collected and evaluated for splenomegaly. Spleen, lung, liver, and heart valve samples were also collected for histopathology and immunocytochemistry. Experiments were conducted in a biosafety level III laboratory.

Histopathology and immunocytochemistry. Lungs, livers, spleens, and heart valves were collected at 14 and 28 days postinfection, fixed for 48 h in 10% buffered formalin, and then stored in 70% ethanol until sectioning. Sectioned tissues were embedded in paraffin, cut to a 5-μm thickness, affixed to slides, and stained with hematoxylin and eosin. The distribution of *C. burnetii* cells was determined by immunocytochemistry, using a rabbit anti-*C. burnetii* Nine Mile phase I antiserum, goat anti-rabbit immunoglobulins, and an avidin-biotin complex (ABC; Vector Laboratories, Burlingame, Calif.).

Measurement of nitric oxide. Cell culture supernatants were collected, and the accumulation of NO_2^-, a stable end product of NO formation, was measured as an indicator of NO production. One hundred microliters of each supernatant plus 100 μl of Griess reagent was incubated at room temperature for 15 min, and then the absorbance was measured at 570 nm. The concentration of NO in the samples was calculated from a standard curve of sodium nitrite (25).

Measurement of hydrogen peroxide. Supernatants were removed from the wells of the plates, and the macrophages were covered with 100 μl of a phenol red-HRPO solution containing stimulants per well. One vertical row served as a blank and contained 100 μl of the phenol red-HRPO solution per well plus 10 μl of 1 N NaOH. The plates were incubated for 1 h at 37°C in 5% CO_2. The reaction was interrupted by the addition of 10 μl of 1 N NaOH per well. After a 3-min interval, the absorbance was read at 630 nm. The concentration of H_2O_2 was calculated from a standard curve of H_2O_2 (47).

Estimation of bacterial doubling times. Doubling times for *C. burnetii* were calculated by using the formula $G = t/[3.3 \times \log(b/B)]$, where G is the generation time, t is the time interval, in hours or minutes, b is the number of bacteria at the end of the interval (144-h time point), and B is the number of bacteria at the beginning of the time interval (96-h time point) (http://textbookofbacteriology.net/growth.html).

Statistics. Significant differences between means were determined by the Student t test by use of the Microsoft Excel statistics analysis pack. Differences were considered statistically significant when P values were <0.05 (indicated by asterisks in the figures). Significant differences between the replication rates were determined by performing a two-tailed Student t test on the average growth rates in each cell type calculated between the 96- and 144-h time points. Differences were considered statistically significant when P values were <0.05.

RESULTS

***C. burnetii* replication rates.** Bacterial loads were determined by real-time PCR on days 2, 4, and 6 postinfection in J774.16 and J774D.9 cells (Fig. 1A) and in PMϕ (Fig. 1B). The estimated doubling times for bacteria were 45 h in J774.16 cells, 20 h in J774D.9 cells, 26 h in wild-type PMϕ, 19 h in p47$^{phox-/-}$ PMϕ, and 17 h in iNOS$^{-/-}$ PMϕ. Although there does appear to be some differential uptake of *C. burnetii* by the various cell types, particularly as shown in Fig. 1B, the ability of a cell to take up bacteria is not directly related to the bacterial growth rate once the bacteria have been phagocytized. Therefore, calculating the doubling times of bacteria in cells demonstrating differential uptake rates is justified. The doubling times of *C. burnetii* were significantly shorter ($P < 0.05$) in cells that were defective for NADPH oxidase or iNOS. These results suggest that wild-type macrophages provide a more growth-restrictive environment than NADPH oxidase- or iNOS-defective macrophages and that the expression of oxygen and nitrogen radicals contributes to this growth suppression. Bacterial doubling times in all cell types were calculated for the interval from 96 to 144 h in an effort to estimate bacterial growth rates during the period of exponential growth.

Effects of nitric oxide and H_2O_2 on *C. burnetii* replication in J774 cell lines. Nitric oxide production by J774 cell lines and primary macrophages was determined by measuring nitrite, a

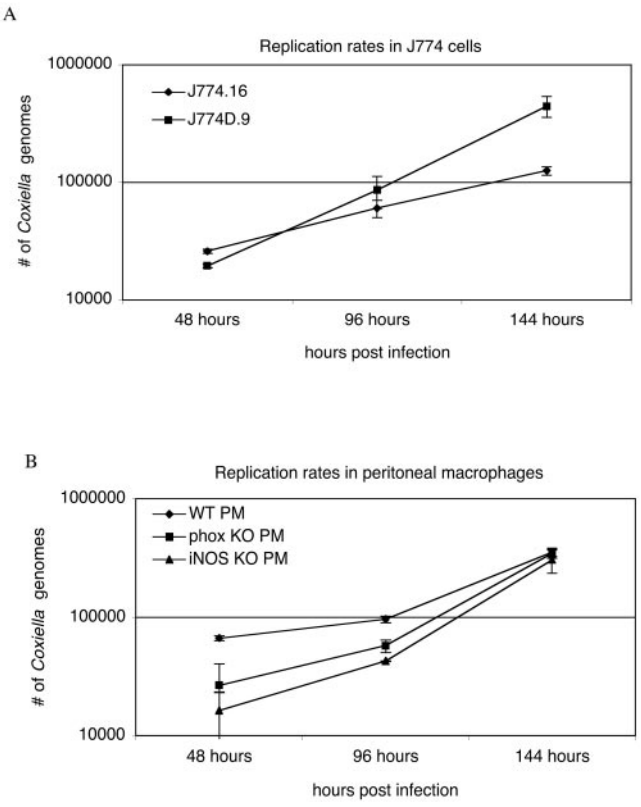

FIG. 1. Estimated generation times for *C. burnetii* in J774 cells and primary murine macrophages. Generation times were calculated by the formula $G = t/[3.3 \times \log(b/B)]$, where G is the generation time, t is the time interval, in hours, b is the number of bacteria at the end of the time interval, and B is the number of bacteria at the beginning of the time interval. (A) Replication rates in J774.16 cells. J774.16, 45 h; J774D.9, 20 h. (B) Replication rates in peritoneal macrophages. Wild-type PMϕ, 26 h; $p47^{phox-/-}$ PMϕ, 19 h; $iNOS^{-/-}$ PMϕ, 17 h. *C. burnetii* replication rates in cells lacking either iNOS or NADPH oxidase were significantly ($P < 0.05$) faster than replication rates in wild-type cells.

stable end product of nitric oxide production. The results show that *C. burnetii* infection alone was not sufficient to stimulate J774.16 or J774D.9 cells to produce significant levels of nitrite (Fig. 2A and B). IFN-γ treatment of infected macrophages resulted in a significant ($P < 0.01$) increase in nitrite production in both macrophage cell lines at 96 and 144 h postinfection. The nitric oxide inhibitor NMMLA was able to suppress nitrite production by 90% in J774.16 cells and by 74% in J774D.9 cells. IFN-γ treatment of infected macrophages also resulted in a significant ($P < 0.05$) production of H_2O_2 by J774.16 cells, but not J774D.9 cells (Fig. 2C and D). The H_2O_2 scavenger catalase reduced H_2O_2 levels by 85% in J774.16 cells. IFN-γ-activated J774.16 cells significantly ($P < 0.05$) inhibited the replication of *C. burnetii* by 144 h postinfection (Fig. 3A). The replication rate was restored to nearly the level in untreated cells in the presence of the iNOS inhibitor NMMLA, suggesting that a nitric oxide-dependent mechanism is involved in controlling *C. burnetii* infections in macrophages. Bacterial replication was restored in J774.16 cells by the addition of catalase. Furthermore, IFN-γ-activated J774D.9 macrophages, which lack a functional respiratory burst, were unable to significantly inhibit *C. burnetii* replication unless an exogenous source of H_2O_2 provided by HX/XO was added (Fig. 3B). Together, these results suggest that an oxygen-radical-dependent mechanism is also involved in controlling *C. burnetii* infections in macrophages.

The viabilities of untreated and treated J774.16 and J774 cells were similar and remained above 86% throughout the experiment, as determined by trypan blue exclusion, indicating that the inhibition of *C. burnetii* replication was not due to host cell death.

Effects of nitric oxide and H_2O_2 on *C. burnetii* replication in primary mouse macrophages. Since low levels of NO and H_2O_2 were still detectable in the presence of iNOS or NADPH oxidase inhibitors, we wanted to further define and clarify the contributions of NO and H_2O_2 to the inhibition of *C. burnetii* replication in vitro. To this end, we performed experiments using primary peritoneal macrophages from $iNOS^{-/-}$, $p47^{phox-/-}$, and wild-type C57BL/6 mice. The cells were infected for 24 h and then left untreated or treated with 100 U of IFN-γ/ml for 5 days. On day 6 postinfection, the bacterial loads in the macrophages, as well as NO and H_2O_2 levels, were determined. As predicted, IFN-γ treatment of the macrophages resulted in an increased production of NO in wild-type and $p47^{phox-/-}$ macrophages but not in $iNOS^{-/-}$ macrophages (Fig. 4A) and in an increased production of H_2O_2 in wild-type and $iNOS^{-/-}$ macrophages but not in $p47^{phox-/-}$ macrophages (Fig. 4B). IFN-γ-treated wild-type, $p47^{phox-/-}$, and $iNOS^{-/-}$ PMϕ all significantly inhibited *C. burnetii* replication compared to untreated PMϕ (Fig. 4C). However, when compared to wild-type PMϕ, $p47^{phox-/-}$ and $iNOS^{-/-}$ PMϕ were less effective at controlling replication, which supports a role for both NO and H_2O_2 in controlling *C. burnetii* infections (Fig. 4C). Peritoneal macrophages lacking NADPH oxidase were not as effective as $iNOS^{-/-}$ PMϕ at controlling replication, suggesting that oxygen radicals play a larger role than NO in inhibiting *C. burnetii* growth in these cells.

Contributions of RNI and ROI in vivo. (i) Clinical signs and gross pathology in mice. To investigate whether oxygen or nitrogen radicals are required for resistance to *C. burnetii* infections in vivo, we infected wild-type, $iNOS^{-/-}$, and $p47^{phox-/-}$ mice intraperitoneally with either 10^4 or 10^7 *C. burnetii* cells and evaluated them for morbidity, pathology, and bacterial distribution at 14 and 28 days postinfection (dpi). At 14 dpi, the $p47^{phox-/-}$ mice who were infected at the 10^7 dose, and to a lesser extent those who were infected at the 10^4 dose, failed to thrive and showed clinical signs of illness, including a hunched posture, a ruffled hair coat, and mild lethargy. No clinical signs were observed for wild-type and $iNOS^{-/-}$ mice who were infected with either dose of *C. burnetii*, except for distended abdomens due to splenomegaly. Pinpoint white foci were seen in the livers of three of four infected (10^7 dose) $p47^{phox-/-}$ and one of four infected (10^7 dose) $iNOS^{-/-}$ mice, suggesting a hematogenous dissemination of the organism. No foci were seen in the livers of the unchallenged controls or wild-type mice at either infectious dose. At 14 dpi, significant increases in spleen mass were observed for all mice who were challenged with 10^4 and 10^7 cells compared to unchallenged controls (Fig. 5A). At the 10^7 dose, spleens from $iNOS^{-/-}$ mice were significantly larger than those from wild-type mice, while $p47^{phox-/-}$ spleens were noticeably smaller. At 28 dpi,

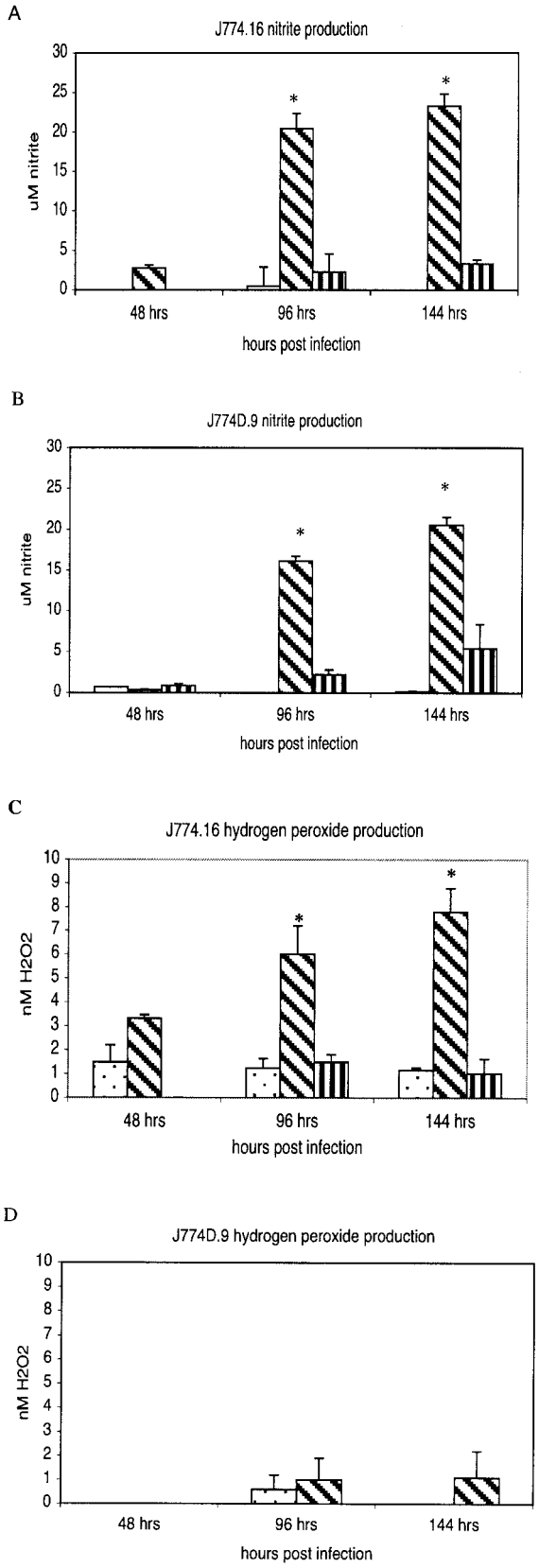

FIG. 2. Nitrite and hydrogen peroxide levels in J774.16 and J774D.9 cells. The cells were infected for 24 h with virulent phase I *C. burnetii* and then were treated with 100 U of murine rIFN-γ/ml in the presence or absence of the iNOS inhibitor NMMLA (1 mM) or the hydrogen peroxide scavenger catalase (100 μM). The stimulation of iNOS was indirectly determined by measuring nitrite, which is a stable end product of nitric oxide production. Hydrogen peroxide levels were determined by measuring the horseradish peroxidase-dependent oxidation of phenol red. (A) Nitrite levels in J774.16 cells. (B) Nitrite levels in J774D.9 cells. (C) Hydrogen peroxide levels in J774.16 cells. (D) Hydrogen peroxide levels in J774D.9 cells. (A and B) Stippled bars, no treatment; diagonally striped bars, treatment with 100 U of IFN-γ/ml; vertically striped bars, treatment with 100 U of IFN-γ/ml and 1 mM NMMLA. (C) Stippled bars, no treatment; diagonally striped bars, treatment with 100 U of IFN-γ/ml; vertically striped bars, treatment with 100 U of IFN-γ/ml and 100 μM catalase. (D) Stippled bars, no treatment; diagonally striped bars, treatment with 100 U of IFN-γ/ml. The results are expressed as means and standard errors for three replicates from two independent experiments. Asterisks indicate significant differences between treated and untreated samples within the same time points.

the $p47^{phox-/-}$ mice who were challenged with either 10^4 or 10^7 *C. burnetii* organisms had begun to resolve the clinical signs of disease, except for the distended abdomens. Infected wild-type and $iNOS^{-/-}$ mice remained clinically normal aside from having distended abdomens. Marked splenomegaly was still evident in all infected mice, with a higher degree of enlargement in mice infected with 10^7 cells (Fig. 5B). Spleens from $p47^{phox-/-}$ mice were significantly larger than those from wild-type or $iNOS^{-/-}$ mice at both infectious doses. Spleens from wild-type and $iNOS^{-/-}$ mice were significantly smaller at 28 dpi than at 14 dpi for mice infected with the 10^4 dose.

(ii) Histopathology. At 14 dpi, the lungs of all mice displayed various degrees of perivascular histiocytic (granulomatous) interstitial pneumonia, with a decrease in the overall airspace. Bronchiolar involvement was occasionally seen, with increased peribronchiolar mononuclear cells and some desquamation of bronchiolar epithelial cells. The severity of the lung changes was greater for mice infected with 10^7 organisms than for mice infected with 10^4 organisms and was greatest for $p47^{phox-/-}$ mice (Table 1). $p47^{phox-/-}$ mice, even those infected at the lower dose, exhibited moderate to severe perivascular histiocytic hepatitis. Lesser changes were noted for $iNOS^{-/-}$ and wild-type mice (Table 1). Marked extramedullary hematopoiesis with myeloid, erythroid, and megakaryocytic hyperplasia, a normal finding in mice, was noted in the livers and spleens of all infected mice compared to uninfected controls. All infected mice had histiocytic splenitis, and again, the $p47^{phox-/-}$ mice displayed the largest degree of change, including rare necrotic foci in the mice infected with the 10^7 dose. The spleens of wild-type mice, and to a slightly lesser extent those of $iNOS^{-/-}$ mice, had diffuse lymphoid hyperplasia. Mild myocarditis and valvular endocarditis were noted for all infected mice. No pathological lesions were noted for control animals.

At 28 dpi, the interstitial pneumonia was resolving in all infected mice, and only a mild decrease in the airspace remained. However, moderate perivascular histiocytic pneumonia was still present in the $p47^{phox-/-}$ mice (Table 1). The livers continued to have granulomatous lesions, with minimal focal necrosis now present in infected animals (10^7 dose). Splenic plasmacytosis was noted for infected wild-type mice, indicating a resolution of the histiocytic splenitis noted at 14 dpi. The spleens of $iNOS^{-/-}$ mice contained more histiocytes

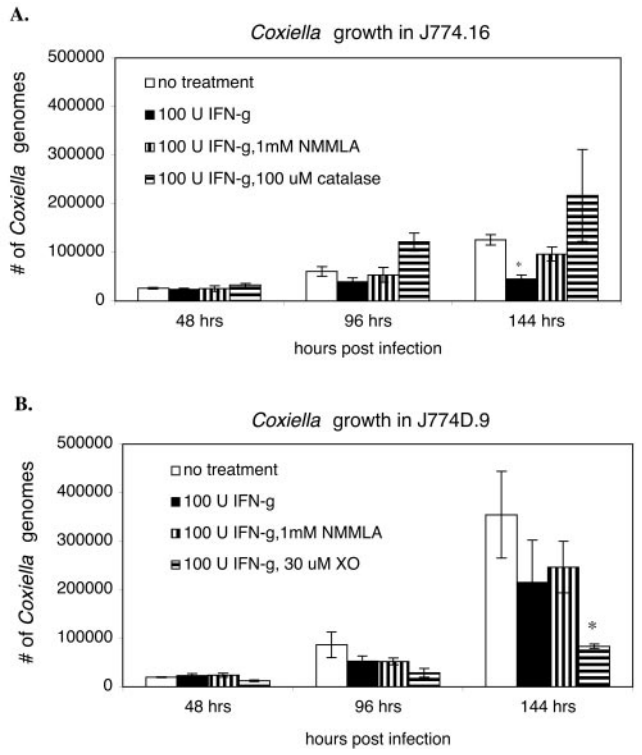

FIG. 3. Effects of IFN-γ treatment on *C. burnetii* growth in J774.16 and J774D.9 cells. At 48, 96, and 144 h postinfection, infected cells were harvested, and the numbers of *C. burnetii* organisms, represented as numbers of *Coxiella* genomes, were determined by real-time PCR. (A) J774.16 cells were infected for 24 h with virulent phase I *C. burnetii* and then were treated with 100 U of murine rIFN-γ/ml in the presence or absence of the iNOS inhibitor NMMLA (1 mM) or the hydrogen peroxide scavenger catalase (100 μM). (B) J774D.9 cells were infected for 24 h with virulent phase I *C. burnetii* and then were treated with 100 U of murine rIFN-γ/ml in the presence or absence of the iNOS inhibitor NMMLA (1 mM) or the ROI donor HX/XO (250 μM/30 μM). The results are expressed as means and standard errors for three replicates from two independent experiments. Asterisks indicate significant differences between treated and untreated samples within the same time points.

and fewer plasma cells than those of wild-type mice. $p47^{phox-/-}$ mice continued to have severe perivascular histiocytic splenitis with marked extramedullary hematopoiesis, minimal focal necrosis, and a lack of follicle organization. Mild myocarditis and valvular endocarditis were noted for all infected mice. Venous microthrombi were present in multiple organs, including lungs, livers, and spleens.

(iii) Immunocytochemistry. *C. burnetii* cells were immunolocalized in lung, liver, spleen, and heart valve samples from wild-type, $iNOS^{-/-}$, and $p47^{phox-/-}$ mice at 14 and 28 days postinfection. At 14 days postinfection, bacteria were detected in all of the tissues from the $iNOS^{-/-}$ and $p47^{phox-/-}$ mice at both challenge doses (Table 2). In general, more organisms were detected in a larger number of tissues in mice receiving the higher challenge dose. No bacteria were detected in the lungs of wild-type mice at either challenge dose. $iNOS^{-/-}$ and $p47^{phox-/-}$ mice were more heavily colonized with *C. burnetii* than wild-type mice, and the bacteria were more widely disseminated in the tissues.

In general, at 28 dpi the bacterial burdens had decreased in all infected animals at both challenge doses compared to those at 14 dpi, with the exception of the heart valves of $iNOS^{-/-}$ and $p47^{phox-/-}$ mice. The heart valves from $iNOS^{-/-}$ and

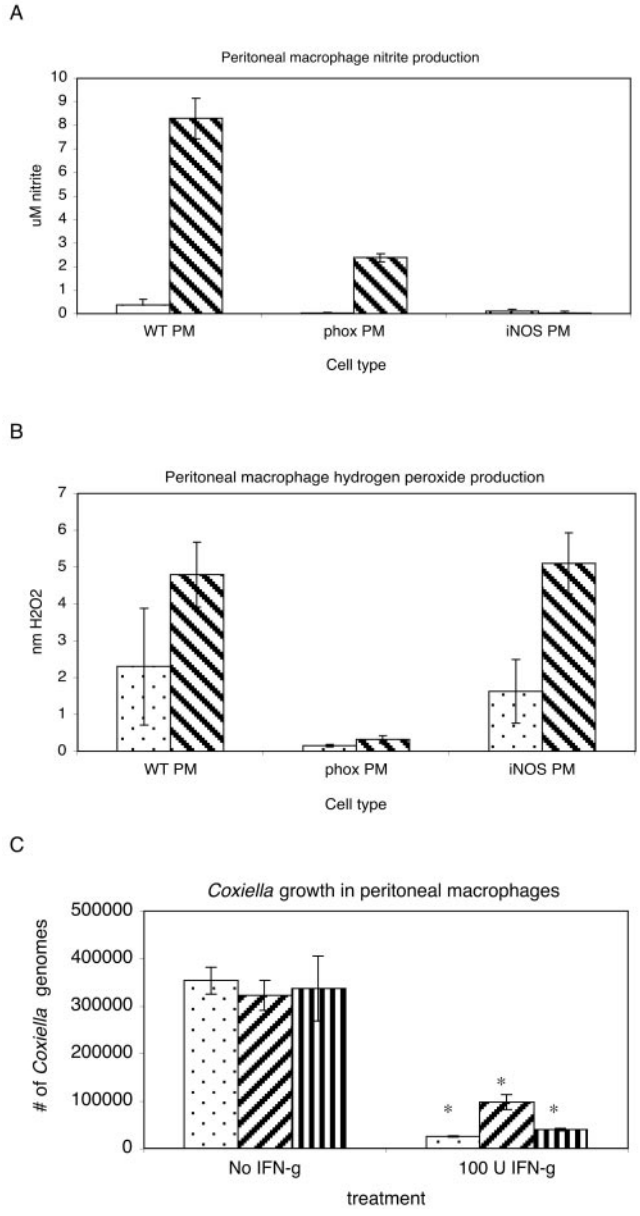

FIG. 4. Growth of virulent phase I *C. burnetii* in primary murine peritoneal macrophages. Macrophages were infected for 24 h with virulent phase I bacteria and then treated for 5 days with or without 100 U of IFN-γ/ml. Nitrite and hydrogen peroxide levels were determined for primary murine peritoneal and bone marrow-derived macrophages. Levels of nitrite (A) and hydrogen peroxide (B) were measured at 144 h postinfection as described for the J774 cell lines. Stippled bars, no treatment; diagonally striped bars, treatment with 100 U of IFN-γ/ml. (C) At 144 h postinfection, peritoneal macrophages were harvested, and the numbers of *C. burnetii* were determined by real-time PCR. Stippled bars, wild type; diagonally striped bars, $p47^{phox-/-}$; vertically striped bars, $iNOS^{-/-}$. The results are expressed as means and standard errors for three replicates. Asterisks indicate significant differences between treated and untreated samples.

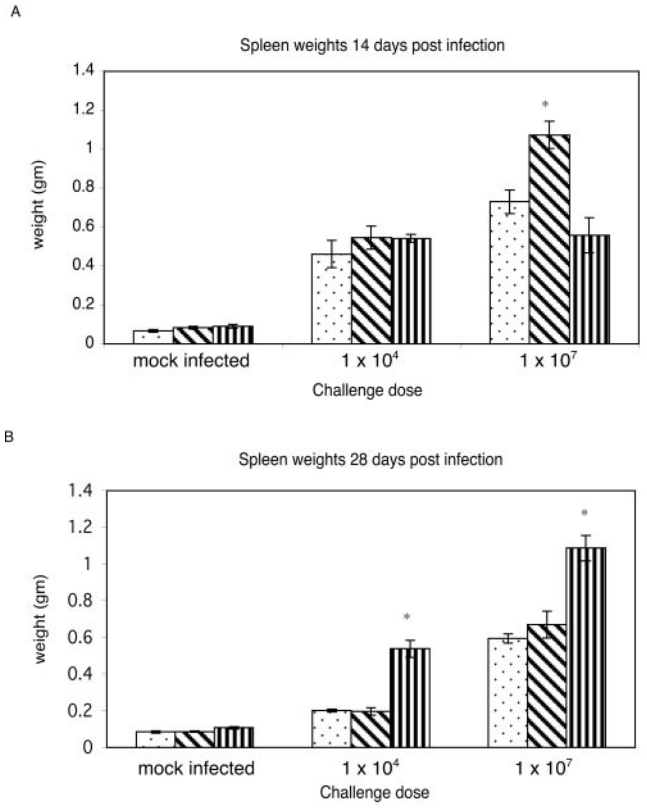

FIG. 5. Splenomegaly in C57BL/6, iNOS$^{-/-}$, and p47$^{phox-/-}$ mice. Mice were challenged intraperitoneally with 10^4 or 10^7 *C. burnetii* cells. At 14 (A) and 28 (B) dpi, spleens were collected and evaluated for splenomegaly. Stippled bars, wild type; diagonally striped bars, iNOS$^{-/-}$; vertically striped bars, p47$^{phox-/-}$. The results are expressed as means and standard errors for four mice. Asterisks indicate significant differences between wild-type and knockout mice.

TABLE 1. Severity of histopathologic changes in selected tissues of mice infected with *C. burnetii*

Tissue or mouse strain	Histopathology score[a] with indicated dose of *C. burnetii*			
	10^4		10^7	
	14 dpi	28 dpi	14 dpi	28 dpi
Lung				
Wild type	2	0	3	1
iNOS KO	3	1	4	1
phox KO	4	2	5	3
Liver				
Wild type	3	2	4	3
iNOS KO	2	1	4	3
phox KO	2	3	5	4
Spleen				
Wild type	3	2	5	4
iNOS KO	3	3	5	4
phox KO	5	5	5	5

[a] Severity was based on the amount of architectural change, cellular infiltration, and the presence or absence of necrosis: 0, none; 1, mild; 2, mild to moderate; 3, moderate; 4, moderate to severe; 5, severe. One section from three mice per group was evaluated. The evaluation of tissue sections was done in a blinded fashion.

TABLE 2. Immunolocalization of *C. burnetii* in mice

Tissue or time after infection	Mouse strain	Immunolocalization of *C. burnetii* at indicated dose[a]	
		10^4	10^7
14 dpi			
Lung	Wild type	−	−
	iNOS KO	+	+
	phox KO	+	+
Liver	Wild type	+	++
	iNOS KO	++	++
	phox KO	+	+++
Spleen	Wild type	++	+++
	iNOS KO	++++	+++
	phox KO	+++	++++
Heart valve	Wild type	+	+
	iNOS KO	+	+
	phox KO	+	++
28 dpi			
Lung	Wild type	−	−
	iNOS KO	+	+
	phox KO	−	+
Liver	Wild type	−	−
	iNOS KO	−	−
	phox KO	−	+
Spleen	Wild type	−	+
	iNOS KO	+	++
	phox KO	+	++
Heart valve	Wild type	+	+
	iNOS KO	++	++
	phox KO	++	+++

[a] −, no organisms present in the tissue section; +, the presence of the organism is rare and focal; ++, few organisms are present, and they are multifocal; +++, many organisms are present, and they are diffuse; ++++, abundance of organisms are present, and they are diffuse. One section from four mice per group was evaluated. The evaluation of tissue sections was done in a blinded fashion.

p47$^{phox-/-}$ mice at both challenge doses contained larger and more numerous foci of infection at 28 dpi than at 14 dpi (Table 2). The distribution of bacteria continued to be more widespread in iNOS$^{-/-}$ and p47$^{phox-/-}$ mice than in wild-type mice in all tissues in which *C. burnetii* was still detected. Figure 6 illustrates the degree of bacterial deposition in the heart valves of mice who were challenged with 10^7 *C. burnetii* cells at 28 days postinfection.

DISCUSSION

C. burnetii is an obligate intracellular pathogen that survives by multiplying in acidified vacuoles of monocytes/macrophages and whose virulence depends on the expression of lipopolysaccharide (LPS). Virulent, phase I bacteria express a complete, or smooth-type, LPS and can be recovered from infected animals, whereas avirulent, phase II bacteria express a truncated, or rough-type, LPS and cannot be recovered from infected animals (29). However, phase I and phase II bacteria are able to replicate in numerous cell types in vitro (4, 13, 20, 31, 32, 54, 57), and several studies have demonstrated the ability of cytokine-activated cells to inhibit phase I and phase II *C. burnetii* replication (20, 32, 54, 57). Recent reports have demonstrated roles for NO in phase II inhibition in L929 murine fibroblasts (32, 57) and a possible role for apoptosis in the elimination of phase I bacteria from human monocytes (20). However, the

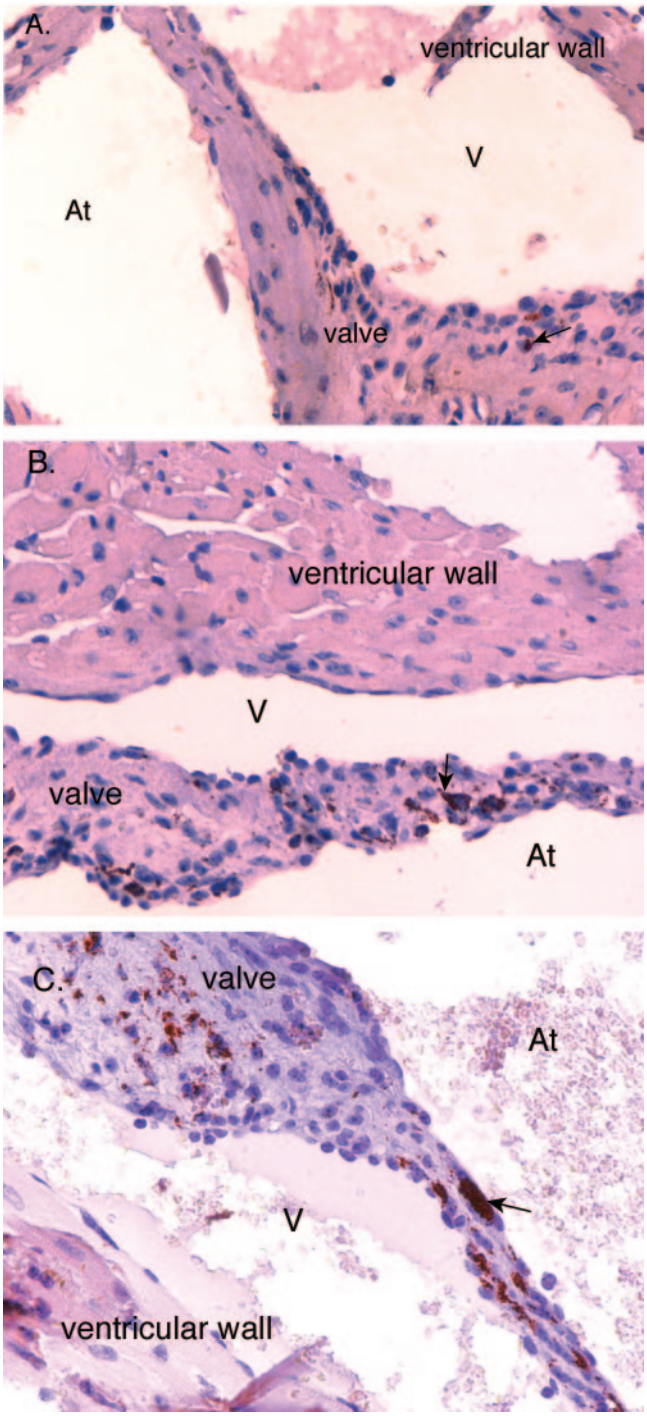

FIG. 6. Immunolocalization of *C. burnetii* in cardiac valve sections from mice challenged with 10^7 *C. burnetii* organisms at 28 days postinfection. *C. burnetii* was detected by the ABC method (Vector Laboratories). (A) Valve section from wild-type mouse; (B) valve section from $iNOS^{-/-}$ mouse; (C) valve section from $p47^{phox-/-}$ mouse. The red to rust-colored deposits represent the presence of *C. burnetii* (arrows denote examples). At, atrial side; V, ventricular side. Magnification, ×40.

potential contributions of ROI in controlling *C. burnetii* infections have not been fully investigated. Zamboni et al. reported that the addition of catalase or superoxide dismutase to phase II-infected bone marrow-derived macrophages had no effect on the relative bacterial loads in untreated or IFN-γ-treated bone marrow-derived macrophages. This report alluded to a finding that *C. burnetii* expresses superoxide dismutase and catalase activities (3) and suggested that these enzyme systems can fully protect *C. burnetii* from ROI (57). However, other pathogens such as *Salmonella enterica* serovar Typhimurium and *Brucella abortus*, which also express superoxide dismutase and catalase enzymes, are susceptible to ROI killing (35, 55), indicating that possessing and expressing ROI defense mechanisms does not necessarily equate protection from the high level of ROI induced by IFN-γ activation. Dellecasagrande et al. have shown that THP-1 monocytes, monocytes from healthy humans, and monocytes from patients suffering from chronic granulomatous disease controlled phase I *C. burnetii* infections despite undetectable levels of RNI or ROI (20). The differences in the capacities of monocytes and macrophages to generate ROI and RNI have been well documented (1, 16); thus, the apoptotic mechanism of controlling *C. burnetii* replication may be a unique but effective alternative for cells such as monocytes that lack the traditional microbicidal capacities of macrophages. Howe et al. proposed that since the phagocytosis of *C. burnetii* does not stimulate a respiratory burst, as defined by the detection of O_2^- (5), *C. burnetii* would not be exposed to toxic peroxynitrite ($ONOO^-$), which is formed through the interaction of superoxide with nitric oxide. However, our results demonstrate that the respiratory burst is activated upon the stimulation of infected macrophages with IFN-γ, as defined by the detection of H_2O_2. We also detected superoxide (O_2^-) produced by IFN-γ activation (data not shown). Recently, Korshunov et al. demonstrated that under acidic conditions, protonated superoxide penetrated lipid membranes at rates similar to water and reported that when *Escherichia coli* CuZnSOD mutants were exposed to superoxide at a low pH, cytosolic fumerase B was damaged (37). Protonated superoxide can also react with itself to form H_2O_2 (42). Therefore, due to the acidic nature of the vacuole in which *C. burnetii* resides, we propose that *C. burnetii* is exposed to a variety of toxic radicals, including O_2^-, NO, H_2O_2, and $ONOO^-$. In this report, we demonstrated that both RNI and ROI contribute to controlling phase I *C. burnetii* infections in vivo as well as in vitro.

The doubling times for *C. burnetii* were determined in cloned and primary macrophages. Bacterial loads were determined at 48, 96, and 144 h postinfection. Twenty-four-hour time points were not taken because the overall goal of the project was to investigate the effects of iNOS and NADPH oxidase on bacterial replication. Thus, the 48-h time point represents the first time point (24 h after treatments) for which comparisons could be made regarding the effects of iNOS and NADPH oxidase on *C. burnetii* growth in untreated and treated cells. The doubling times were calculated for untreated samples. Doubling times were determined by using the 96- and 144-h time points as time zero and the end time, respectively, in an effort to calculate doubling times only during the period of exponential growth. The use of these time points also diminished any effects of initial bacterial uptake on the calcu-

lated growth rates. The replication rates of *C. burnetii* were approximately two times faster in NADPH oxidase- or iNOS-defective macrophages, suggesting that RNI and ROI may be partially responsible for the slower growth rates in immunocompetent cells. These findings are similar to those of a previous report that demonstrated that phase II bacterial loads were larger in unstimulated primary macrophages treated with iNOS-inhibiting agents than in unstimulated, untreated primary macrophages (57). One possibility for the extended doubling times observed in NADPH oxidase and iNOS competent cells is that *C. burnetii* may devote more energy to up-regulating genes that are necessary to detoxify low levels of reactive nitrogen and oxygen intermediates that may be present in resting macrophages. For example, stationary-phase infectious *Legionella pneumophila* has been demonstrated to express several virulence traits, including catalase and superoxide dismutase, that are thought to be important for *L. pneumophila* to establish an infection (10, 11, 53).

To determine the effects of iNOS and NADPH oxidase on phase I *C. burnetii* infections in vitro, we monitored bacterial replication in IFN-γ-activated J774 cell lines that differed in the ability to produce ROI. IFN-γ-activated J774.16 macrophages significantly inhibited bacterial replication, and this inhibition was reversed by the addition of either the iNOS inhibitor NMMLA or the H_2O_2 scavenger catalase, suggesting that RNI and ROI both contribute to controlling *C. burnetii* infections. Interestingly, the inhibition of iNOS did not fully rescue the growth defect of *C. burnetii* in IFN-γ-treated macrophages, whereas the inhibition of H_2O_2 did appear to fully rescue and possibly promote bacterial replication, suggesting that ROI, and H_2O_2 in particular, may play a larger role than RNI in controlling infections in these cells. Similar effects were seen by Feng and Walker in cytokine-treated *Rickettsia conorii*-infected human umbilical vein endothelial cells (22). The addition of NMMLA to cytokine- and chemokine-treated infected human umbilical vein endothelial cells resulted in an approximately 85% recovery of bacterial growth, while the addition of catalase led to an approximately 160% recovery. This apparent augmentation of replication may be a result of relieving the stress of endogenous ROI as well as exogenous ROI. IFN-γ-activated J774D.9 macrophages, which lack a functional NADPH oxidase, only significantly inhibited bacterial replication when an exogenous source of H_2O_2 was added, which also indicates the importance of ROI in controlling infections. The finding that the inhibition of either iNOS or NADPH oxidase resulted in a rescue of growth suggests that the control of *C. burnetii* is in part due to the synergistic effects of RNI and ROI.

In an effort to substantiate the in vitro findings from the cloned cell lines, we employed primary macrophages that differed in the ability to produce ROI and RNI, which allowed us to avoid the use of inhibitors or donors that may have had incomplete or nonspecific effects. Although IFN-γ-activated $iNOS^{-/-}$ and $p47^{phox-/-}$ macrophages did not produce significant amounts of NO or H_2O_2, respectively, they did inhibit bacterial replication significantly more than untreated controls. These data suggest that in addition to RNI- and ROI-dependent mechanisms, the activation of macrophages results in bacteriostatic mechanisms that are independent of iNOS and NADPH oxidase. Several investigators have demonstrated that IFN-γ activation results in iron limitation and tryptophan starvation, which serve to inhibit the growth of other intracellular pathogens (23, 26, 39, 46). Interestingly, activated $iNOS^{-/-}$ peritoneal macrophages were only slightly less effective while activated $p47^{phox-/-}$ peritoneal macrophages were significantly less effective at controlling infections than activated wild-type peritoneal macrophages, suggesting that ROI may play a more significant role in controlling *C. burnetii* infections than RNI in these cells.

This hypothesis was further supported by the finding that mice lacking iNOS were less effective at controlling *C. burnetii* infections than wild-type mice and that NADPH oxidase-deficient mice were even less effective than $iNOS^{-/-}$ mice. Although a dose-dependent splenomegaly was apparent in all infected mice, the phenotypes of the $iNOS^{-/-}$ and $p47^{phox-/-}$ mice were markedly different from that of wild-type mice. The $iNOS^{-/-}$ mice appeared to have an initial period of increased susceptibility followed by a period of recovery, as indicated by the presence of liver foci and significant splenomegaly at 14 dpi and by no liver foci and splenomegaly similar to that of wild-type mice at 28 dpi. The $p47^{phox-/-}$ mice appeared to have a more severe phenotype than the $iNOS^{-/-}$ mice. At 14 dpi, more of these mice possessed liver foci and developed clinical signs of illness, and by 28 dpi these mice demonstrated significantly more splenomegaly than wild-type mice. These data support the general hypothesis that ROI play a more significant role in protection than RNI in the infection of mice.

The findings that both $iNOS^{-/-}$ and $p47^{phox-/-}$ mice were more susceptible to infection than wild-type mice and that either iNOS or H_2O_2 inhibitors were able to rescue growth defects in vitro indicate that RNI and ROI both contribute, possibly in a synergistic fashion, to controlling *C. burnetii* infections. Synergy between RNI and ROI can occur through various interactions. For example, the interaction of NO with O_2^- results in the formation of toxic peroxynitrite ($ONOO^-$), which has the ability to directly oxidize DNA bases and sulfhydryl groups and to cause lipid peroxidation (41). Nitric oxide has also been demonstrated to inactivate Fe-S-containing enzymes such as aconitase, resulting in the release of Fe^{2+}, which can then interact with H_2O_2 as part of the Haber-Weiss reaction to form toxic hydroxyl radicals that are also capable of oxidizing proteins, DNA, and lipids (28, 41). The synergistic effects of RNI and ROI on the inhibition of pathogens have been previously demonstrated. Pacelli et al. reported that hydrogen peroxide-dependent killing of *E. coli* increased 1,000-fold in the presence of nitric oxide and could be prevented by the chelation of iron (45). Another study, by Darrah et al., demonstrated that mice lacking iNOS or $gp91^{phox}$ were more susceptible to lethal challenges of *Rhodococcus equi* than wild-type mice and also demonstrated in vitro that efficient killing of *R. equi* cells was observed in the presence of peroxynitrite but not in the presence of nitric oxide or superoxide alone (19). The passage of protonated superoxide into the *C. burnetii*-containing vacuole could potentiate the formation of $ONOO^-$. It was previously demonstrated that NO contributed to the inhibition of *C. burnetii* replication in cytokine-stimulated L929 cells by preventing the formation of large replicative vacuoles (32). Further investigation is required to determine if ROI are also involved in this mechanism. Finally, the finding that an iNOS- and NADPH oxidase-independent mechanism(s) may

also be involved in controlling *C. burnetii* infections illustrates the probable complexity and possible redundancy of the innate immune response to bacterial infections.

The dissemination and lack of clearance of *C. burnetii* in the heart valves of iNOS$^{-/-}$ and p47$^{phox-/-}$ mice suggest that RNI and ROI may play critical roles in the prevention of *C. burnetii*-associated endocarditis, which is the major clinical presentation of chronic Q fever. The development of chronic Q fever has often been associated with immunodeficiency (15, 48, 50) and has only been demonstrated in lab animals that were either immunosuppressed or had previously damaged heart valves. Atzpodien et al. reported the dissemination of *C. burnetii* by 10 days postinfection in cardiac valves of mice treated with cyclophosphamide, and more recently, Andoh et al. demonstrated that SCID mice infected with *C. burnetii* developed endocarditis resembling the pathology seen in human Q fever endocarditis (6, 8). Those studies involved widespread and nonspecific immunosuppression affecting several potential immune system mechanisms at various levels. In this study, we have demonstrated that the specific lack of a functional iNOS or NADPH oxidase contributes to the colonization and persistence of *C. burnetii* in cardiac valves. It is possible that the *C. burnetii*-associated endocarditis documented in previous studies may have been in part due to the lack of adequately activated macrophages and to a poor stimulation of iNOS and NADPH oxidase. Further characterization of these and other mouse strains is required to adequately evaluate their usefulness as models of Q fever endocarditis.

ACKNOWLEDGMENTS

This work was supported by Public Health Service grants AI37744 and AI448191 from the National Institute of Allergy and Infectious Diseases.

We thank Vernon Tesh and Renée Tsolis for their critical reviews of the manuscript.

REFERENCES

1. **Adams, D. O., and T. A. Hamilton.** 1984. The cell biology of macrophage activation. Annu. Rev. Immunol. **2:**283–318.
2. **Adams, L. B., M. C. Dinauer, D. E. Morgenstern, and J. L. Krahenbuhl.** 1997. Comparison of the roles of oxygen and nitrogen intermediates in the host response to mycobacterium tuberculosis using transgenic mice. Tuber. Lung Dis. **78:**237–246.
3. **Akporiaye, E. T., and O. G. Baca.** 1983. Superoxide anion production and superoxide dismutase and catalase activities in *Coxiella burnetii*. J. Bacteriol. **154:**520–523.
4. **Akporiaye, E. T., J. D. Rowatt, A. A. Aragon, and O. G. Baca.** 1983. Lysosomal response of a murine macrophage-like cell line persistently infected with *Coxiella burnetii*. Infect. Immun. **40:**1155–1162.
5. **Akporiaye, E. T., D. Stefanovich, V. Tsosie, and G. Baca.** 1990. *Coxiella burnetii* fails to stimulate human neutrophil superoxide anion production. Acta Virologica **34:**64–70.
6. **Andoh, M., T. Naganawa, A. Hotta, T. Yamaguchi, H. Fukushi, T. Masegi, and K. Hirai.** 2003. SCID mouse model for lethal Q fever. Infect. Immun. **71:**4717–4723.
7. **Asher, M. S., P. B. Jahrling, D. G. Harrington, R. A. Kishimoto, and V. G. McGann.** 1980. Mechanisms of protective immunogenicity of microbial vaccines: effects of cyclophosphamide pretreatment in Venezuelan encephalitis, Q fever, and tularemia. Clin. Exp. Immunol. **41:**225–236.
8. **Atzpodien, E., W. Baumgartner, A. Artelt, and D. Thiele.** 1994. Valvular endocarditis occurs as a part of a disseminated *Coxiella burnetii* infection in immunocompromised Balb/cj (H-2^d) mice infected with the Nine Mile isolate of *C. burnetii.* J. Infect. Dis. **170:**223–226.
9. **Babudieri, C.** 1959. Q fever: a zoonosis. Adv. Vet. Sci. **5:**81–84.
10. **Bandyopadhyay, P., B. Byrne, Y. Chan, M. S. Swanson, and H. M. Steinman.** 2003. *Legionella pneumophila* catalase-peroxidases are required for proper trafficking and growth in primary macrophages. Infect. Immun. **71:**4526–4535.
11. **Bandyopadhyay, P., and H. M. Steinman.** 2000. Catalase-peroxidases of *Legionella pneumophila*: cloning of the *katA* gene and studies of KatA function. J. Bacteriol. **182:**6679–6686.
12. **Beauchamp, C., and I. Fridovich.** 1970. A mechanism for the production of ethylene from methional. The generation of the hydroxyl radical by xanthine oxidase. J. Biol. Chem. **245:**4641–4646.
13. **Beron, W., M. G. Gutierrez, M. Rabinovitch, and M. I. Colombo.** 2002. *Coxiella burnetii* localizes in a Rab7-labeled compartment with autophagic characteristics. Infect. Immun. **70:**5816–5821.
14. **Brennan, R. E., and J. E. Samuel.** 2003. Evaluation of *Coxiella burnetii* antibiotic susceptibilities by real-time PCR assay. J. Clin. Microbiol. **41:**1869–1874.
15. **Capo, C., Y. Zaffran, F. Zugan, P. Houpikian, D. Raoult, and J. L. Mege.** 1996. Production of interleukin-10 and transforming growth factor β by peripheral blood mononuclear cells in Q fever endocarditis. Infect. Immun. **64:**4143–4150.
16. **Cohn, Z. A.** 1978. The activation of mononuclear phagocytes: fact, fancy, future. J. Immunol. **121:**813–816.
17. **Clark, R. A.** 1990. The human neutrophil respiratory burst oxidase. J. Infect. Dis. **161:**1140–1147.
18. **Damiani, G., C. Kiyotaki, W. Soeller, M. Sasada, J. Peisach, and B. R. Bloom.** 1980. Macrophage variants in oxygen metabolism. J. Exp. Med. **152:**808–822.
19. **Darrah, P. A., M. K. Hondalus, Q. Chen, H. Ischiropoulos, and D. M. Mosser.** 2000. Cooperation between reactive oxygen and nitrogen intermediates in killing of *Rhodococcus equi* by activated macrophages. Infect. Immun. **68:**3587–3593.
20. **Dellacasagrande, J., C. Capo, D. Raoult, and J.-L. Mege.** 1999. IFN-γ-mediated control of *Coxiella burnetii* survival in monocytes: the role of cell apoptosis and TNF. J. Immunol. **176:**2259–2265.
21. **Fang, F. C.** 1997. Mechanisms of nitric oxide related antimicrobial activity. J. Clin. Investig. **99:**2818–2825.
22. **Feng, H. M., and D. H. Walker.** 2000. Mechanisms of intracellular killing of *Rickettsia conorii* in infected human endothelial cells, hepatocytes, and macrophages. Infect. Immun. **68:**6729–6736.
23. **Gebran, S. J., Y. Yamamoto, C. Newton, T. W. Klein, and H. Friedman.** 1994. Inhibition of *Legionella pneumophila* growth by gamma interferon in permissive A/J mouse macrophages: role of reactive oxygen species, nitric oxide, tryptophan, and iron (III). Infect. Immun. **62:**3197–3205.
24. **Goldberg, M., L. S. Belkowski, and B. R. Bloom.** 1990. Regulation of macrophage function by interferon-gamma. Somatic cell genetic approaches in murine macrophage cell lines to mechanisms of growth inhibition, the oxidative burst, and expression of the chronic granulomatous disease gene. J. Clin. Investig. **85:**563–569.
25. **Granger, D. L., J. B. Hibbs, and L. M. Broadnax.** 1991. Urinary nitrate excretion in relation to murine macrophage activation: influence of dietary L-arginine and oral N^G-monomethyl-L-arginine. J. Immunol. **146:**1294–1302.
26. **Gupta, S. L., J. M. Carlin, P. Pyati, W. Dai, E. R. Pfefferkorn, and M. J. Murphy, Jr.** 1994. Antiparasitic and antiproliferative effects of indoleamine 2,3-dioxygenase enzyme expression in human fibroblasts. Infect. Immun. **62:**2277–2284.
27. **Haas, A., and W. Goebel.** 1992. Microbial strategies to prevent oxygen-dependent killing by phagocytes. Free Radic. Res. Commun. **16:**137–157.
28. **Haber, F., and J. Weiss.** 1934. The catalytic decomposition of hydrogen peroxide by iron salts. Proc. R. Soc. Lond. A **147:**332–351.
29. **Hackstadt, T., M. G. Peacock, P. J. Hitchcock, and R. L. Cole.** 1985. Lipopolysaccharide variation in *Coxiella burnetii*: interstrain heterogeneity in structure and antigenicity. Infect. Immun. **48:**359–365.
30. **Hibbs, J. B., Jr., Z. Vavrin, and R. R. Taintor.** 1987. L-Arginine is required for expression of the activated macrophage effector mechanism causing selective metabolic inhibition in target cells. J. Immunol. **138:**550–565.
31. **Hinrichs, D. J., and T. R. Jerrells.** 1976. In vitro evaluation of immunity to *Coxiella burnetii*. J. Immunol. **117:**996–1003.
32. **Howe, D., L. F. Barrows, N. M. Lindstrom, and R. A. Heinzen.** 2002. Nitric oxide inhibits *Coxiella burnetii* replication and parasitophorous vacuole maturation. Infect. Immun. **70:**5140–5147.
33. **Izzo, A. A., and B. A. Marmion.** 1993. Variation in interferon-γ responses to *Coxiella burnetii* antigens with lymphocytes from vaccinated and naturally infected subjects. Clin. Exp. Immunol. **94:**507–514.
34. **Jackett, P. S., V. R. Aber, and D. B. Lowrie.** 1978. Virulence and resistance to superoxide, low pH, and hydrogen peroxide among strains of *Mycobacterium tuberculosis*. J. Gen. Microbiol. **104:**37–45.
35. **Jiang, X., B. Leonard, R. Bensen, and C. L. Baldwin.** 1993. Macrophage control of *Brucella abortus*: role of reactive oxygen intermediates and nitric oxide. Cell. Immunol. **151:**309–319.
36. **Kishimoto, R. A., H. Rozmiarek, and R. W. Larson.** 1978. Experimental Q fever infection in congenitally athymic nude mice. Infect. Immun. **22:**69–71.
37. **Korshunov, S. S., and J. A. Imlay.** 2002. A potential role for periplasmic superoxide dismutase in blocking the penetration of external superoxide into the cytosol of gram-negative bacteria. Mol. Microbiol. **43:**95–106.
38. **MacMicking, J. D., R. J. North, R. LaCourse, J. S. Mudgett, S. K. Shah, and C. F. Nathan.** 1997. Identification of nitric oxide synthase as a protective locus against tuberculosis. Proc. Natl. Acad. Sci. USA **94:**5243–5248.

39. **Manor, E., and I. Sarov.** 1990. Inhibition of *Rickettsia conorii* growth by recombinant tumor necrosis factor alpha: enhancement of inhibition by gamma interferon. Infect. Immun. **58:**1886–1890.
40. **Marrie, T. J.** 1990. Epidemiology of Q fever, p. 49–70. *In* T. J. Marrie (ed.), Q fever, vol. 1. The disease. CRC Press, Boca Raton, Fla.
41. **Miller, R. A., and B. E. Britigan.** 1995. The formation and biological significance of phagocyte-derived oxidants. J. Investig. Med. **43:**39–49.
42. **Miller, R. A., and B. E. Britigan.** 1997. Role of oxidants in microbial pathophysiology. Clin. Microbiol. Rev. **10:**1–18.
43. **Murray, H. W., and D. M. Cartelli.** 1983. Killing of intracellular *Leishmania donovani* by human mononuclear phagocytes: evidence for oxygen-dependent and -independent leishmanicidal activity. J. Clin. Investig. **72:**32–39.
44. **Murray, H. W., and C. F. Nathan.** 1999. Macrophage microbicidal mechanisms in vivo: reactive nitrogen versus oxygen intermediates in the killing of intracellular visceral *Leishmania donovani*. J. Exp. Med. **189:**741–746.
45. **Pacelli, R., D. A. Wink, J. A. Cook, M. C. Krishna, W. DeGraff, N. Friedman, M. Tsokos, A. Samuni, and J. B. Mitchell.** 1995. Nitric oxide potentiates hydrogen peroxide-induced killing of *Escherichia coli*. J. Exp. Med. **182:** 1469–1479.
46. **Pfefferkorn, E. R.** 1984. Interferon-gamma blocks the growth of *Toxoplasma gondii* in human fibroblasts by inducing the host cell to degrade tryptophan. Proc. Natl. Acad. Sci. USA **81:**908–912.
47. **Pick, E.** 1986. Microassays for superoxide and hydrogen peroxide production and nitroblue tetrazolium reduction using an enzyme immunoassay microplate reader. Methods Enzymol. **132:**407–421.
48. **Raoult, D.** 1990. Host factors in the severity of Q fever. Ann. N. Y. Acad. Sci. **590:**33–38.
49. **Raoult, D.** 1993. Treatment of Q fever. Antimicrob. Agents Chemother. **37:**1733–1736.
50. **Raoult, D., P. Brouqui, B. Marchou, and J.-A. Gastaut.** 1992. Acute and chronic Q fever patients with cancer. Clin. Infect. Dis. **14:**127–130.
51. **Raoult, D., P. Houpikian, H. Tissot Dupont, M. J. Riss, J. Arditi-Djiane, and P. Brouqui.** 1999. Comparison of 2 regimens containing doxycycline and ofloxacin or hydroxychloroquine. Arch. Intern. Med. **159:**167–273.
52. **Scanga, C. A., V. P. Mohan, K. Tanaka, D. Alland, J. L. Flynn, and J. Chan.** 2001. The inducible nitric oxide synthase locus confers protection against aerogenic challenge of both clinical and laboratory strains of *Mycobacterium tuberculosis* in mice. Infect. Immun. **69:**7711–7717.
53. **St. John, G., and H. M. Steinman.** 1996. Periplasmic copper-zinc superoxide dismutase of *Legionella pneumophila*: role in stationary-phase survival. J. Bacteriol. **178:**1578–1584.
54. **Turco, J., H. A. Thompson, and H. Winkler.** 1984. Interferon-γ inhibits growth of *Coxiella burnetii* in mouse fibroblasts. Infect. Immun. **45:**781–783.
55. **Vazquez-Torres, A., J. Jones-Carson, P. Mastroeni, H. Ischiropoulos, and F. C. Fang.** 2000. Antimicrobial actions of the NADPH phagocyte oxidase and inducible nitric oxide synthase in experimental salmonellosis. I. Effects on microbial killing by activated peritoneal macrophages in vitro. J. Exp. Med. **192:**227–236.
56. **Weiss, S. J.** 1986. Oxygen, ischemia and inflammation. Acta Physiol. Scand. **548**(Suppl.)**:**9–37.
57. **Zamboni, D. S., and M. Rabinovitch.** 2003. Nitric oxide partially controls *Coxiella burnetii* phase II infection in mouse primary macrophages. Infect. Immun. **71:**1225–1233.

Editor: F. C. Fang